Original Article

Mitophagy-mediated inflammation and oxidative stress contribute to muscle wasting in cancer cachexia

Zhige Zhang,† Shanjun Tan,† Shuhao Li, Yuxi Cheng, Junjie Wang, Hao Liu, Mingyue Yan, and Guohao Wu*

Department of General Surgery/Shanghai Clinical Nutrition Research Center, Zhongshan Hospital, Fudan University, 180 Fenglin Road, Xuhui District, Shanghai 200032, China

(Received 11 January, 2023; Accepted 12 February, 2023; Released online in J-STAGE as advance publication 13 June, 2023)

Cancer cachexia is commonly seen in patients with malignant tumors, which usually leads to poor life quality and negatively affects long-term prognosis and survival. Mitochondria dysfunction and enhanced autophagy are well-established to play an important role in skeletal muscle wasting. However, whether mitophagy is engaged in the pathogenesis of cancer cachexia requires further investigation. This study comprised a clinical study and animal experimentation. Clinical data such as CT images and laboratory results were obtained and analyzed. Then mice model of cancer cachexia and mitophagy inhibition were established. Data including skeletal muscle mass and function, mitochondria structure and function, inflammatory factors as well as ROS concentration. Mitophagy was enhanced in cancer cachexia patients with increased inflammatory factors. Greater disruption of skeletal muscle fiber and mitochondria structure were seen in cancer cachexia, with a higher level of inflammatory factors and ROS expression in skeletal muscle. Meanwhile, ATP production was undermined, indicating a close relationship with mitophagy, inflammation, and oxidative stress in the skeletal muscle of cancer cachexia mice models. In conclusion, mitophagy is activated in cancer cachexia and may play a role in skeletal muscle atrophy, and inflammation and oxidative stress might participate in mitophagy-related skeletal muscle injury.

***Key Words*: cancer cachexia, mitophagy, skeletal muscle wasting, inflammation, oxidative stress**

Cancer cachexia is a syndrome caused by multiple factors, characterized by different degrees of skeletal muscle wasting and dysfunction,[1] causing impairment during daily activities, motor function degeneration and a negative effect on the quality of life, worsening long-term prognosis.[2,3] Therefore, the mechanism and the treatment of skeletal muscle loss in cancer cachexia warrant further research.

An increasing body of evidence suggests that autophagic-lysosomal system (ALS) overactivation is responsible for skeletal muscle protein degradation in cancer cachexia patients.[4,5] Autophagy is a cleansing process in different varieties of cells; damaged or aging proteins and organelles automatically form into autophagosomes and are subject to degeneration by lysosomes to maintain an overall metabolic balance.[6,7] However, in wasting diseases like cancer cachexia, unduly ALS activation causes body composition wasting, negative energy balance and skeletal muscle loss.[8] As a special form of autophagy, mitophagy is characterized by the removal of mitochondria.[9] Previous studies have revealed that mitophagy is accomplished through different pathways, Parkin-dependent and non-Parkin protein-dependent pathways such as Bcl2 and adenovirus E1B19 kDa interacting protein 3 (BNIP3) and FUN14 domain containing 1 (FUNDC1) protein pathways documented in different diseases.[10–12]

As the major factory of energy production, the overall wellness of mitochondria is critical for physical maintenance. Mitochondrial fission and fusion simultaneously exist in different cells, and a dynamic mitochondrial metabolism is balanced with mitophagy.[13,14] It has been established that the dynamic balance between mitochondrial generation and degradation is critical for quality maintenance, and dynamic dysfunction might be closely related to skeletal muscle loss in cancer cachexia.[15,16] Although the relationship between mitophagy and cancer cachexia is not clear, recent studies revealed that mitophagy is promoted in diseases such as sepsis and renal diseases.[17,18] Enhanced inflammation and oxidative stress have been related to dysregulated mitophagy, which leads to organ dysfunction and systemic damage.[19,20]

Therefore, the current study aims at exploring mitophagy activity in the skeletal muscle of cancer cachexia subjects and whether inflammation and oxidative stress are related to dysregulated mitophagy, hoping to identify a new target for the treatment of this particular patient population.

Methods

Patients. This study was approved by the Ethics committee of Zhongshan Hospital, Fudan University. Thirty one patients with gastrointestinal cancer indicated for surgery from June 2021 to June 2022 were prospectively recruited. The inclusion criteria were as follows: (1) aged from 18 to 90 years old; (2) diagnosed with gastrointestinal cancer; (3) patients with surgical indications; (4) written consent was provided. The exclusion criteria included: (1) patients that underwent emergency surgery; (2) patients with severe comorbidities such as heart failure and sepsis; (3) weight loss unrelated to cancer; (4) contraindicated for surgery. General characteristic includes disease type, age, height, body weight, body mass index (BMI), weight loss in recent 6 months, NRS-2002 score and comorbidities. Examination information included: albumin, inflammatory factors, computed tomography (CT) scan images, and clinicopathological features.

After being recruited, patients were divided into a control group and a cancer cachexia group. The cachexia diagnostic criteria were as follows: (1) >5% weight loss over the past 6 months; (2) BMI <20 kg/m^2 and >2% weight loss over the past 6

*To whom correspondence should be addressed.
E-mail: prowugh@163.com
†Equally contributed to this work.

doi: 10.3164/jcbn.23-1

months; (3) Absence of sarcopenia and >2% weight loss over the past 6 months. Rectus abdominis muscle specimens were acquired during surgery. A 1 cm^3 muscle specimen was obtained from each patient using sharp dissection and stored at −80°C until further use.

Animal models. Balb/c mice were obtained from the central laboratory and divided into 4 groups: a control group (C, $n = 5$), mitophagy inhibited group (M, $n = 5$), cancer cachexia group (CC, $n = 5$), and cancer cachexia with mitophagy inhibited group (CCM, $n = 5$). Mice in the control group did not receive any treatment. Mice in the mitophagy-inhibited group were injected with mitochondrial division inhibitor 1 (mdivi-1) while the cancer cachexia group was inoculated with tumor cells. The cancer cachexia with mitophagy-inhibited group was inoculated with tumor cells and injected with mdivi-1. After a week of acclimation, C26 cells were injected subcutaneously on the first day of the experiment to establish the cancer cachexia model. Mdivi-1 was used daily through intraperitoneal injection since day 14 with 30 mg/kg body weight to inhibit mitophagy. During modeling, all groups were weighed every two days, and grip strength and autonomous activity were tested every week. All four groups were anesthetized on day 21 and sacrificed to harvest the gastrocnemius muscle. Part of the muscle specimen was divided and fixed in fixation liquid. The remaining tissues were stored at −80°C until further usage. This study was approved by the Ethics committee of Zhongshan Hospital, Fudan University.

CT image analysis. CT scan was performed before surgery, and the images of the third lumbar vertebra layer were extracted. Skeletal muscle were selected through tissue-specific Hounsfield units (HU) thresholds from −29 to +150 HU, and the area of skeletal muscle was documented and normalized by height and represented as skeletal muscle index (SMI, cm^2/m^2).

Skeletal muscle fiber area. After formalin fixation and paraffin embedding, the gastrocnemius muscle was cut into cross-sections and was observed under light microscopy after hematoxylin and eosin staining. Fiber areas in cross-sections of ≥150 fibers were measured using ImageJ software ver. 1.53t.

Ultrastructural analyses. After glutaraldehyde-osmium fixation and upon embedding, the gastrocnemius muscle was longitudinally sectioned. Skeletal fiber arrangement, mitochondrial diameter and structure were assessed by a scanning Transmission Electron Microscope (HT7800; HITACHI, Tokyo, Japan).

Western blot analysis. Fifty mg skeletal muscle was divided and added into RIPA buffer, phosphatase inhibitors, and protease. Proteins were extracted and quantified to 5 μg/ml with BCA protein quantitation Kit, then were separated by 7.5% and 12.5% SDS-PAGE, electrophoretically transferred to a polyvinylidene difluoride membrane and blocked by BSA. After incubation overnight at 4°C with anti-LC3A/B, anti-Bnip3 (1:1,000, Cell Signaling Technology, Danvers, MA) and anti-PINK1 (1:1,000; Abcam, Cambridge, UK), membranes were washed by TBST and incubated with anti-mouse or anti-rabbit Ig. Immunoreactive bands were visualized by enhanced chemiluminescence solution (Thermo Scientific, Waltham, MA). Band quantitative analysis was performed using ImageJ software ver. 1.53t.

Inflammatory factors. Protein was extracted from gastrocnemius muscles, and analyzed by mouse IL-6 Elisa Kit (H007-1-2; Nanjing Jiancheng, Nanjing, China) and mouse TNF-α Elisa Kit (HH052-1; Nanjing Jiancheng), according to the manufacturer's instructions, and the results were analyzed by GraphPad Prism 8 software.

ATP concentration. Gastrocnemius muscles were lyzed with RIPA buffer and a mixture of phosphatase inhibitors and protease. The ATP assay kit (A095-1-1; Nanjing Jiancheng) was utilized, and through phosphorylation of glycerol, samples were quantified by colorimetric means (570 nm). ATP concentration analysis was conducted following the instructions of the ATP assay kit, and the results were analyzed by GraphPad Prism 8 software.

Immunohistochemistry. Gastrocnemius muscles were formalin-fixed and paraffin-embedded. After endogenous peroxidase inactivation, heat-induced antigen retrieval and serum incubation, samples were incubated overnight at 4°C with primary antibodies Anti-Fbx32 and Anti-MuRF1 (1:400, Abcam) and

Table 1. Clinical characteristics of patients with digestive tumor

Characteristic		Overall patients ($n = 31$)	Control ($n = 18$)	Cancer cachexia ($n = 13$)	p value
Sex	Male	19 (61.3)	11 (61.1)	8 (61.5)	0.98
	Female	12 (38.7)	7 (38.9)	5 (38.5)	
Age (year)			63.8 ± 11.6	64.8 ± 8.9	0.8
Comorbidity	Yes	14 (45.2)	8 (44.4)	6 (46.2)	0.93
	No	17 (54.8)	10 (55.6)	7 (53.8)	
Height (cm)			165.0 ± 10.3	164.5 ± 7.5	0.88
Weight (kg)			66.3 ± 9.9	58.9 ± 7.5	0.03*
BMI (kg/m^2)			24.3 ± 2.7	21.7 ± 2.2	
NRS-2002 score	<3	13 (41.9)	13 (72.2)	0 (0)	<0.01*
	≥3	18 (58.1)	5 (27.8)	13 (100)	
Albumin (g/L)			41.0 ± 3.0	38.4 ± 3.6	0.02*
SMI (cm^2/m^2)			46.9 ± 8.8	37.9 ± 7.0	0.01
Histological types	Poor differentiated	4 (12.9)	3 (16.7)	1 (76.9)	0.84
	Poor-medium differentiated	13 (41.9)	7 (38.9)	6 (46.1)	0.69
	Medium differentiated	13 (41.9)	7 (38.9)	6 (46.1)	0.69
	High differentiated	1 (3.2)	1 (5.5)	0 (0)	1
Clinical stages	I	3 (9.7)	3 (16.7)	0 (0)	0.25
	II	19 (61.3)	11 (61.1)	8 (61.5)	1
	III	6 (19.4)	3 (16.7)	3 (23.1)	0.68
	IV	3 (9.7)	1 (5.6)	2 (15.4)	0.56

Values are means ± SD or n (%). Differences between groups were tested by one-factor ANOVA followed by least significant difference post hoc tests. * indicates $p<0.05$.

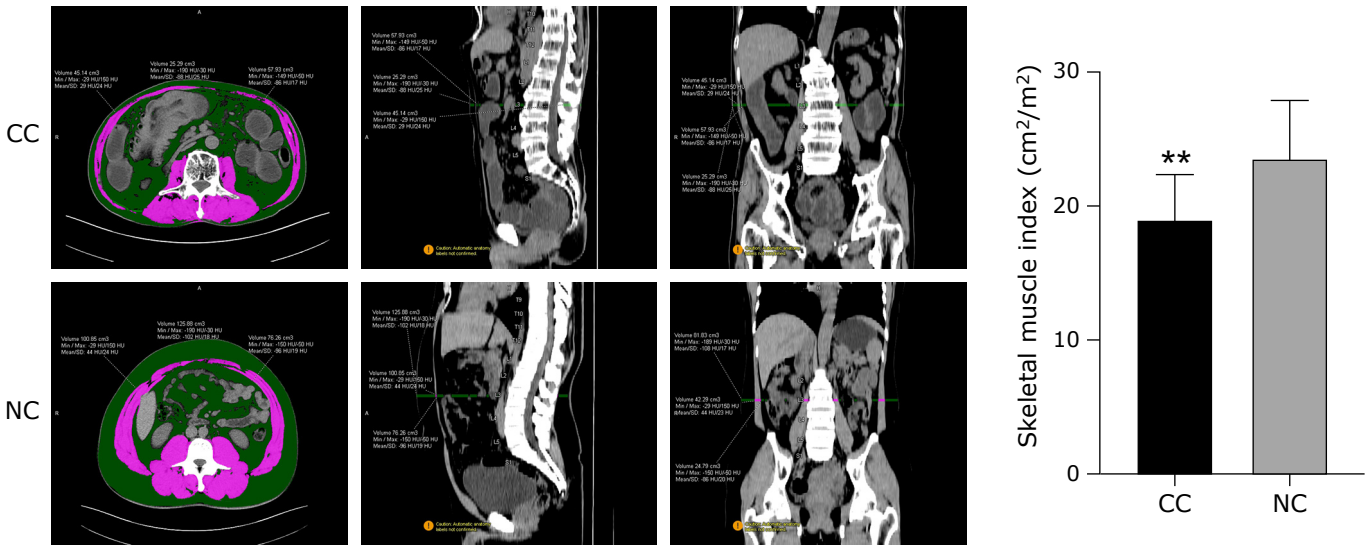

Fig. 1. Skeletal muscle mass in the two groups, **Significant difference at $p<0.01$ between two groups. NC, non-cancer cachexia group; CC, cancer cachexia group; SMI, skeletal muscle index.

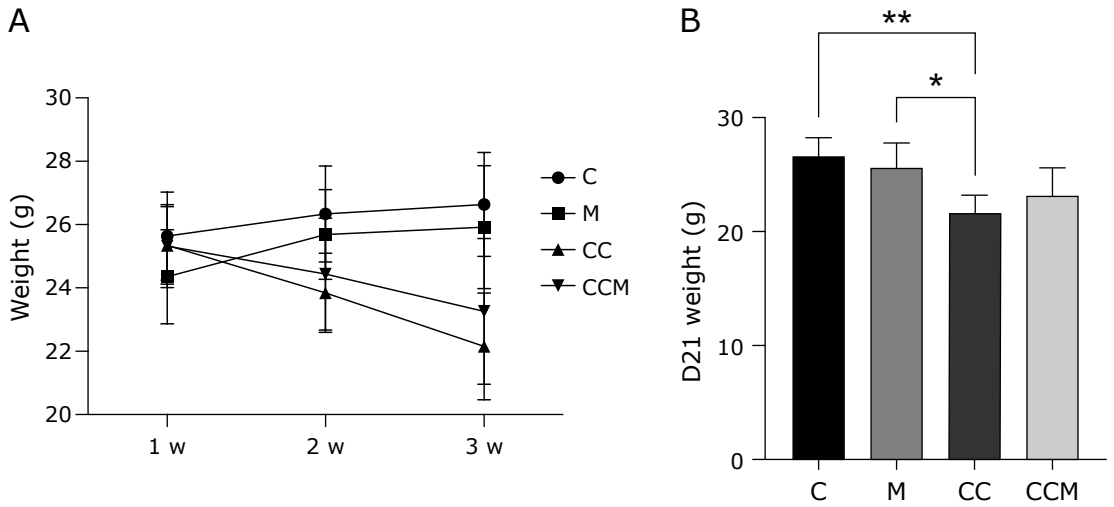

Fig. 2. (A) Weight changes of subjects in the groups during 3 weeks of modeling. (B) Body weight at day 21 in each group. *Significant difference at $p<0.05$ between indicated groups, **Significant difference at $p<0.01$ between indicated groups. C, control group; M, mitophagy inhibited group; CC, cancer cachexia group; CCM, cancer cachexia + mitophagy inhibited group.

incubated in goat anti-mouse IgG antibody. Then sections were incubated in an avidin-biotin complex at 37°C for 30 min and nuclear stained with hematoxylin. After treatment with diaminobenzene, sections were dehydrated with ethanol and treated with xylene. ImageJ software ver. 1.53t was used for data analysis.

Skeletal muscle specimens stored at −80°C were sliced by cryostat and stained with Dihydroethidium (DHE). After incubating at 37°C for 30 min, 4',6-diamidino-2-phenylindole (DAPI; G1012; Servicebio, Wuhan, China) was used for nuclear counterstaining and sections were mounted with Antifade Mounting Medium (G1401; Servicebio), observed with a Zeiss 780 laser scanning confocal microscope (Carl Zeiss Microscopy GmbH, Jena, Germany). Quantitative analysis was performed using ImageJ software ver. 1.53t.

Statistical analysis. Quantitative data from different groups were expressed as means ± SD (normally distributed) or median (nonnormally distributed) and were compared by one-way ANOVA and Bonferroni post hoc test. Categorical data were expressed as numbers and percentages, while the Chi-squared test or Fisher's exact probability tests were used to compare differences between groups. A p value <0.05 was statistically significant. Statistical analyses were performed with GraphPad Prism 8 software (GraphPad Software, San Diego, CA) and SPSS Statistics ver. 23.0 (IBM, New York, NY).

Results

Patients characteristics. Thirty one patients with gastrointestinal cancer were enrolled and divided into cancer cachexia ($n = 13$) and control ($n = 18$) groups. The clinical characteristics are shown in Table 1. The skeletal muscle area in the cancer cachexia group exhibited a significant decline in CT imaging (Fig. 1A). The mean age of the patients was 64 years, and the SMI of the cancer cachexia group was significantly lower than the control group (Fig. 1B).

doi: 10.3164/jcbn.23-1

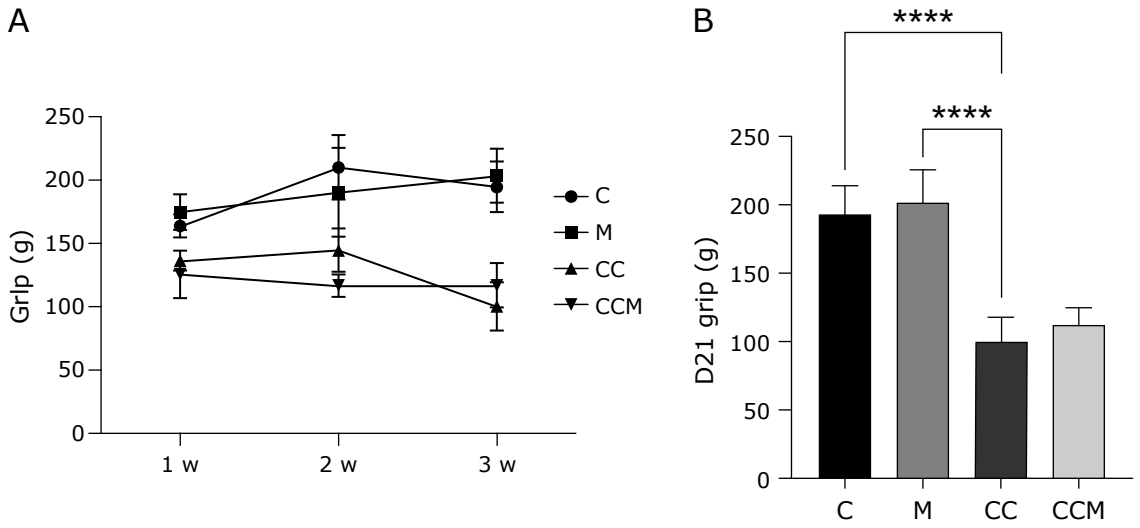

Fig. 3. (A) Grip changes of subjects in the groups during 3 weeks of modeling. (B) Mean ± SD grip at day 21 of each group. ****Significant difference at $p<0.001$ between indicated groups. C, control group; M, mitophagy inhibited group; CC, cancer cachexia group; CCM, cancer cachexia + mitophagy inhibited group.

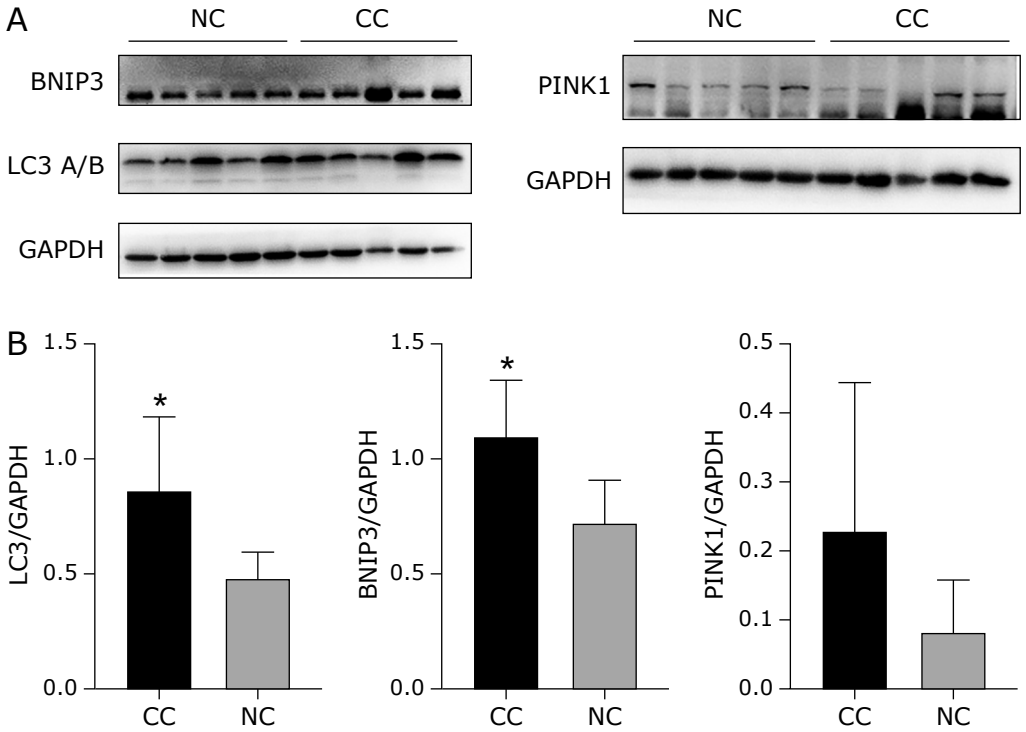

Fig. 4. Expression of mitophagy markers in rectus abdominis muscles of patients in the groups. LC3A/B, bnip3 and PINK1 protein expression was evaluated by Western blotting: protein expression was normalized using GAPDH as a loading control. *Significant difference at $p<0.05$ between two groups. NC, non-cancer cachexia group; CC, cancer cachexia group; LC3, microtubule associated protein 1 light chain 3 β; BNIP3, Bcl2 and adenovirus E1B19 kDa interacting protein 3; PINK1, PTEN-induced putative kinase 1.

Cancer cachexia model establishment. To establish a cancer cachexia model, C26 cells were injected subcutaneously in Balb/c mice. During the process, grip strength tests were performed weekly, and subjects loaded with tumors exhibited a gradual decline in muscle strength (Fig. 2A). Compared to the C and M groups, the CC and CCM groups exhibited lower grip strength at the end of the experiment (Fig. 2B). Meanwhile, we found that the autonomic activity of subjects with cancer cachexia declined weekly (Fig. 3A), exhibiting less activity compared to the C and M groups (Fig. 3B). These findings indicated that the cancer cachexia model was established successfully.

Expression of mitophagy in skeletal muscles. Western blot was performed to assess the expression of mitophagy protein in the rectus abdominis muscle of patients. PINK1 and Bnip3 proteins represent different pathways of mitophagy initiation, and LC3A/B protein was used to measure ALS marker expression. Bnip3 and LC3A/B protein expression were significantly higher

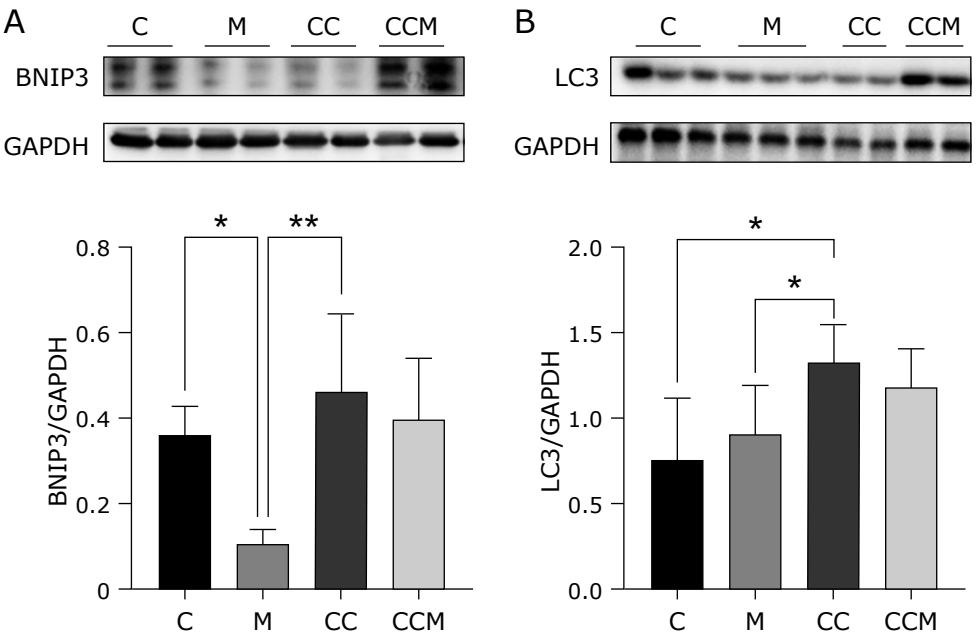

Fig. 5. Expression of mitophagy markers in gastrocnemius muscles of subjects in the groups. Bnip3 and LC3 protein expression was evaluated by Western blotting: protein expression was normalized using GAPDH as a loading control. *Significant difference at $p<0.05$ between two groups. **Significant difference at $p<0.01$ between two groups. C, control group; M, mitophagy inhibited group; CC, cancer cachexia group; CCM, cancer cachexia + mitophagy inhibited group; LC3, microtubule associated protein 1 light chain 3 β; BNIP3, Bcl2 and adenovirus E1B19 kDa interacting protein 3.

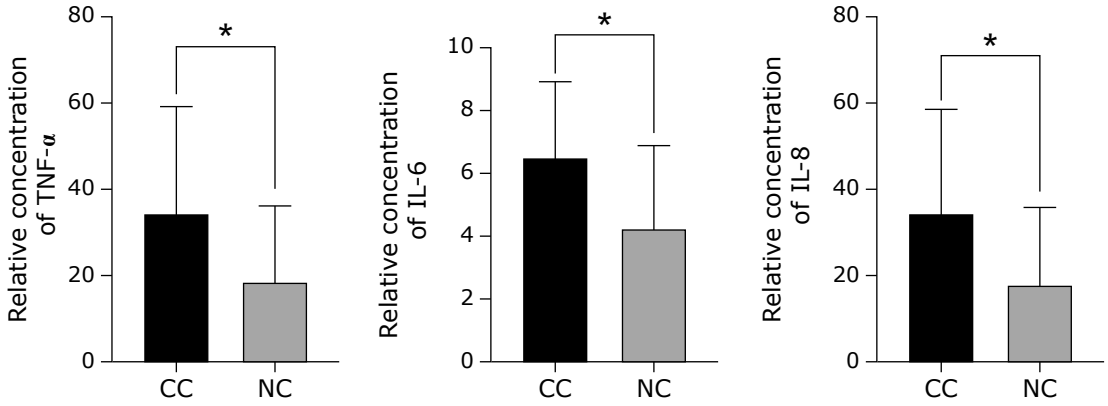

Fig. 6. Expression of inflammatory factors in serum of patients in the groups. TNF-α, IL-6, and IL-6 expression was evaluated by ELISA. *Significant difference at $p<0.05$ between two groups. NC, non-cancer cachexia group; CC, cancer cachexia group.

in the cancer cachexia group, while no significant difference was observed in the PINK1 protein (Fig. 4), indicating mitophagy is partially activated in rectus abdominis muscles of patients with cancer cachexia.

Gastrocnemius muscle specimens were acquired, and Western blots were performed to assess the expression of mitophagy in animal models. BNIP3 and LC3 proteins expression in the C group were relatively higher than the other 3 groups, and mice injected with Mdivi-1 exhibited lower expression of BNIP3 proteins (Fig. 5), indicating Mdivi-1 could suppress mitophagy activity. Mitophagy in cancer cachexia models was activated, similar to findings in human skeletal muscle.

Expression of inflammatory factors. To evaluate systemic inflammatory reaction, we obtained blood samples preoperatively and found that TNF-α, IL-6, and IL-8 were elevated in the cancer cachexia group (Fig. 6). The results suggested that the inflammatory reaction was overactivated in patients with cancer cachexia.

ELISA was performed to determine the relative expression of IL-6 and TNF-α in the skeletal muscle of animal models. CC group showed a higher concentration of inflammatory factors than the CCM group and the other 2 groups (Fig. 7), indicating the enhanced mitophagy activity was closely related to the inflammatory reaction in skeletal muscle with cancer cachexia.

Skeletal muscle fiber area. Gastrocnemius muscle sections stained with hematoxylin and eosin were observed under an optical microscope. Cross-sectional observations showed that skeletal muscle fibers were sparsely arranged and less regulated in the CC group compared with the other 3 groups (Fig. 8A). Meanwhile, the muscle fiber cross-sectional area was significantly decreased in the CC group (Fig. 8B). Although the CCM group exhibited a loss of skeletal muscle fiber, the severity was milder compared to the CC group, indicating mitophagy overactivation.

doi: 10.3164/jcbn.23-1

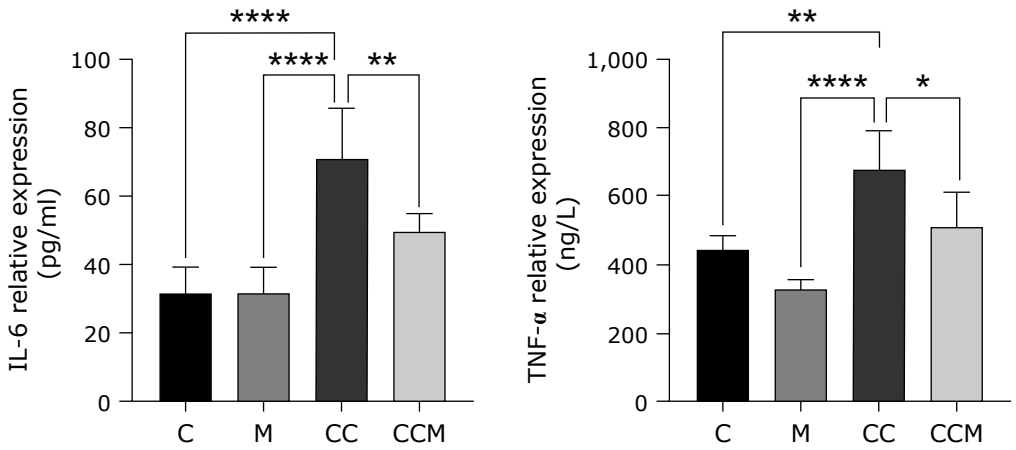

Fig. 7. Expression of inflammatory factors in gastrocnemius muscles of subjects in the groups. IL-6 and TNF-α expression was evaluated by ELISA. *Significant difference at $p<0.05$ between two groups. **Significant difference at $p<0.01$ between two groups. ****Significant difference at $p<0.001$ between two groups. C, control group; M, mitophagy inhibited group; CC, cancer cachexia group; CCM, cancer cachexia + mitophagy inhibited group.

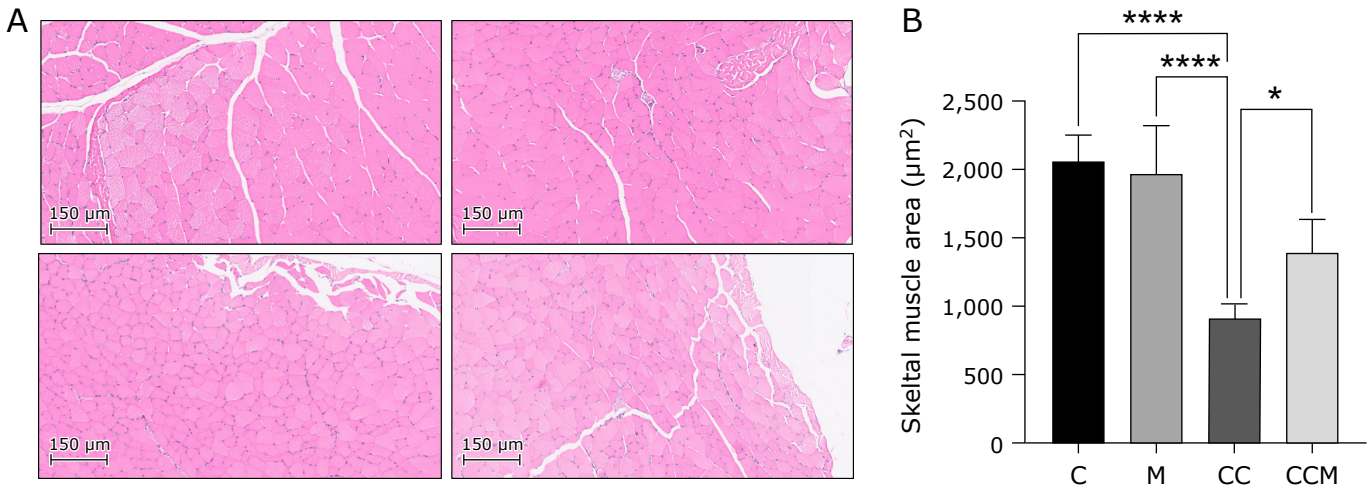

Fig. 8. Muscle fiber morphology and cross-sectional area of gastrocnemius muscle fibers of subjects in each group. (A) Representative hematoxylin and eosin–stained gastrocnemius muscle sections from each group. In cross-sections, the gastrocnemius muscle fibers were round and compactly arranged in the C and M groups. Atrophy was observed in the CC and CCM groups, which manifested as sparsely arranged shrinking triangles or polygons. (B) Mean ± SD cross-sectional areas of muscle fibers in the gastrocnemius muscle of each group. *Significant difference at $p<0.05$ between indicated groups. ****Significant difference at $p<0.001$ between indicated groups. C, control group; M, mitophagy inhibited group; CC, cancer cachexia group; CCM, cancer cachexia + mitophagy inhibited group.

Expression of skeletal muscle atrophy protein. We performed immunohistochemistry to assess the expression of Murf1 and atrogin1 protein to observe the degree of skeletal muscle atrophy. The results showed that the expression of Murf1 in the CC group was higher than the other 3 groups (Fig. 9A), while atrogin1 protein exhibited higher expression (Fig. 9B). This finding suggested that mitophagy overactivation might be related to skeletal muscle atrophy.

Ultrastructural muscle architecture. The structure and arrangement of skeletal muscle fiber and mitochondria of gastrocnemius muscles were observed under electron microscopy. The CC group exhibited a disorganized sarcomere arrangement with swollen and broken mitochondria, while mitochondria in the M and CCM groups were merged and presented with clearer cristae (Fig. 10), indicating that cancer cachexia has a negative influence on mitochondria structure.

Mitochondrial function. ATP concentration was used to mirror the mitochondrial energy supply. Compared to the other 3 groups, the concentration of ATP was significantly decreased in the CC group, and energy deficiency was less obvious in the CCM group (Fig. 11A).

It is widely acknowledged that ROS immunofluorescence can be used to visualize the cellular levels of oxidative stress. ROS were highly expressed in the CC group compared to the CCM group (Fig. 11B), indicating enhanced mitophagy activity might be closely related to oxidative stress in skeletal muscle with cancer cachexia.

Discussion

In our study, patients with cancer cachexia presented a loss of skeletal muscle and activation of mitophagy, as well as systemic inflammatory reactions. Based on these findings, we established a cancer cachexia animal model, and through Mdivi-1 intraperitoneal injection, mitophagy activity was suppressed in M and CCM groups to observe the relationship between skeletal muscle

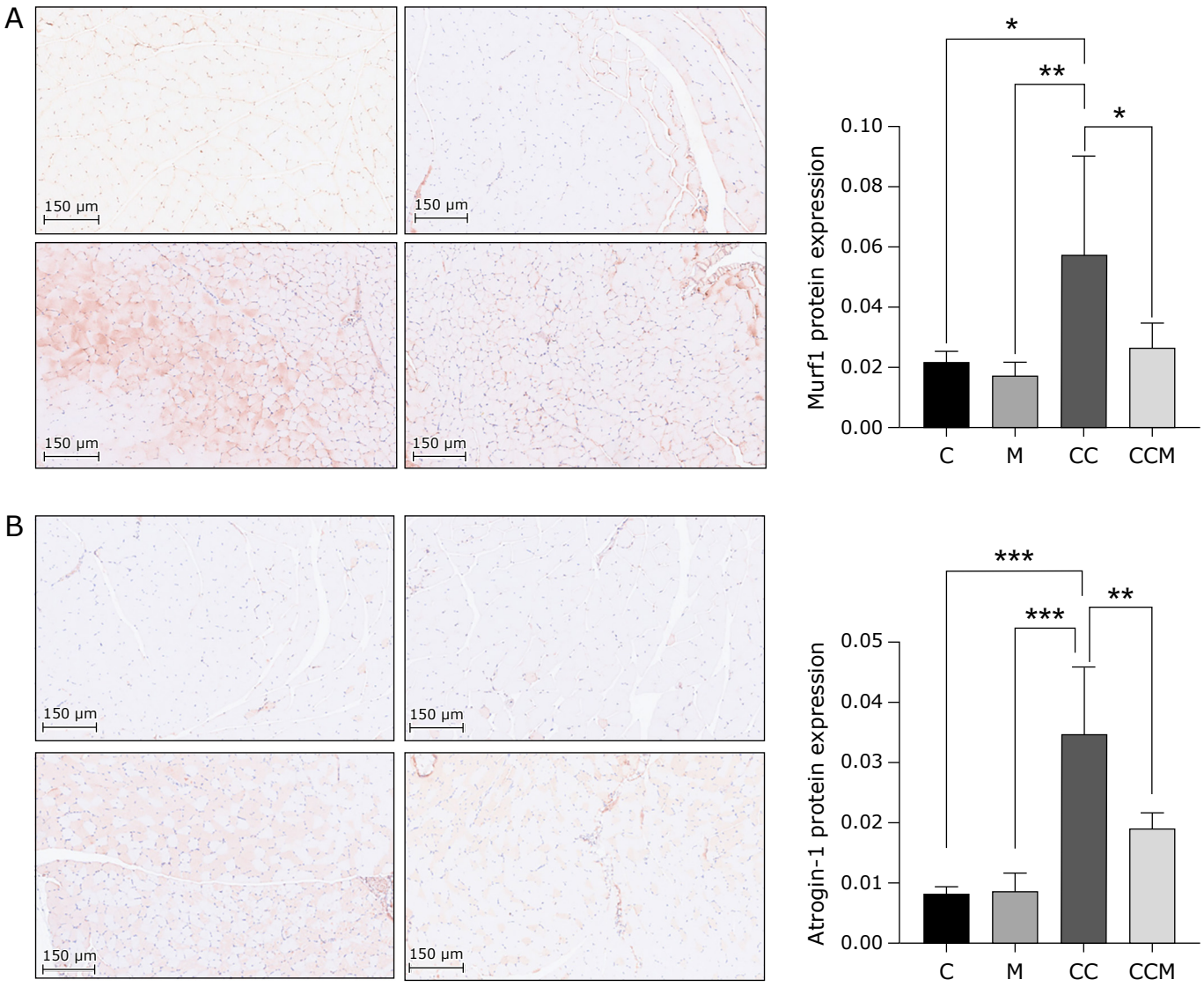

Fig. 9. Muscle atrophy protein expression of gastrocnemius muscle fibers of subjects in the groups. (A) IHC of gastrocnemius muscle sections from each group. Murf1 and atrogin1 protein was observed in the CC and CCM groups. (B) Mean ± SD of Murf1 and atrogin1 protein expression in the gastrocnemius muscle of each group. *Significant difference at $p<0.05$ between indicated groups. **Significant difference at $p<0.01$ between indicated groups. ***Significant difference at $p<0.005$ between indicated groups. C, control group; M, mitophagy inhibited group; CC, cancer cachexia group; CCM, cancer cachexia + mitophagy inhibited group.

dysfunction and mitophagy in cancer cachexia. Furthermore, inflammation and oxidative stress in skeletal muscle with cancer cachexia were assessed to primarily explore the mechanism of mitophagy-induced skeletal muscle injury.

Patients with gastrointetinal cancer were recruited in this study. To ensure accuracy of our findings, strict inclusion and exclusion criteria were established to minimize the influence of confounding factors on skeletal muscle structure and function disability, enhanced inflammatory reaction and oxidative reaction. Patients recruited in the control group and cancer cachexia group exhibited no significant difference in age, sex and other basic characteristics. Compared with the control group, patients in the cancer cachexia group exhibited lower serum albumin and higher NRS-2002 score. Meanwhile, CT scan images of the third lumbar vertebra layer showed that SMI in the cancer cachexia group was significantly lower than the control group, indicating skeletal muscle loss in patients with cancer cachexia, which is in accordance with previous studies. It has been established that autophagy activity is increased in the skeletal muscle of patients with cancer cachexia, which was also observed in our study with an elevation of LC3A/B protein. In recent years, PINK1 and BNIP3 proteins have been associated with important mitophagy pathways.[21,22] The present study showed that BNIP3 protein expression was elevated in the skeletal muscle, while PINK1 protein levels were comparable between the two groups, consistent with a previous study,[23] suggesting that mitophagy is unduly expressed in the skeletal muscle of patients with cancer cachexia through different pathways. We also found that compared to the control group, the cancer cachexia group exhibited a higher level of inflammatory factors. Previous study have revealed that preemptive administration of TNF-α antibody might mitigate cancer cachexia, indicating an important role of inflammatory factors in the development of cancer cachexia.[24] There is a growing consensus that increased inflammatory reaction and mitophagy activation occur separately.[23,25,26] In our study, mitophagy and systemic inflammatory reaction were exacerbated

doi: 10.3164/jcbn.23-1

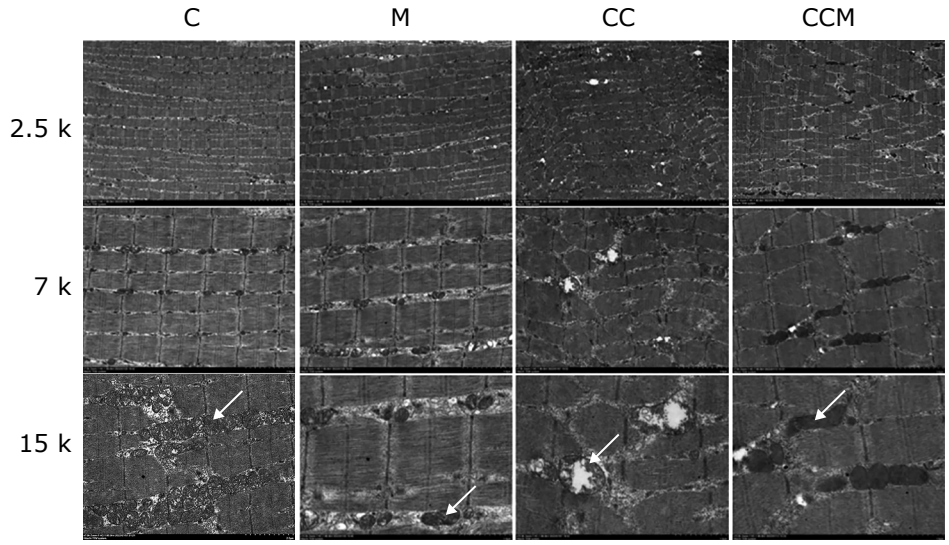

Fig. 10. Representative ultrastructural images of the vastus lateralis in the groups. Myofilaments were oriented in parallel with well-organized sarcomeres and mitochondria was regularly aligned on both sides of the Z-lines in C and M group muscles. Disorganized sarcomere arrangement with swelled and broken mitochondria were seen in CC group while mitochondria in M group and CCM group were merged and presented a clearer crest. Mitochondria in different groups were pointed with white arrows. C, control group; M, mitophagy inhibited group; CC, cancer cachexia group; CCM, cancer cachexia + mitophagy inhibited group.

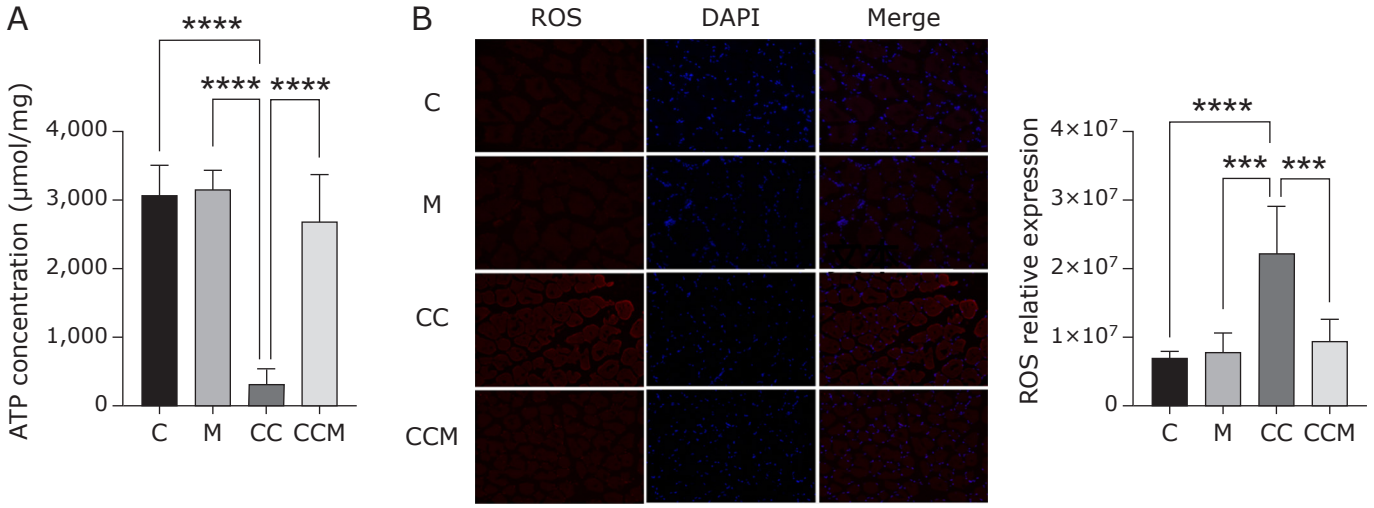

Fig. 11. Mitochondria function of gastrocnemius muscle fibers of subjects in the groups. (A) ATP concentration in the gastrocnemius muscle of each group. (B) ROS expression in the gastrocnemius muscle of each group. ***Significant difference at $p<0.005$ between indicated groups. ****Significant difference at $p<0.001$ between indicated groups. C, control group; M, mitophagy inhibited group; CC, cancer cachexia group; CCM, cancer cachexia + mitophagy inhibited group. ATP, adenosine triphosphate; ROS, reactive oxygen species; DAPI, 4',6-diamidino-2-phenylindole.

at the same time, emphasizing the need for future research on their relationship.

The cancer cachexia model and mitophagy suppression model were established and we observed alterations in their skeletal muscle structure, functions, inflammation, and oxidative stress. Patients with cancer cachexia exhibited smaller skeletal muscle fiber areas and higher expression of skeletal muscle atrophy protein MURF1 and atrogin-1. By injecting Mdivi-1 consecutively for a week, mitochondria number and structure were rescued compared to the C group. ATP concentration was elevated and oxidative stress was suppressed in CCM group though with cancer cachexia, inflammatory factors IL-6 and TNF-α were also decreased comparing to CC group. These results indicate that mitophagy is unduly stimulated in the skeletal muscle of subjects with cancer cachexia, accompanied by an inflammatory reaction and oxidative stress, which might be responsible for skeletal muscle loss and dysfunction to a certain extent.

Although we revealed a potential link between mitophagy and skeletal muscle loss in cancer cachexia, some limitations and shortcomings were found in this study. Indeed, it has been established that Mdivi-1 inhibits mitophagy and suppresses the Drp1 protein.[27,28] However, little is known about the influence of mitochondrial dynamics, nor is it clear how mitophagy influences inflammation and oxidative stress, warranting further study.[29,30] Further research based on cell experiments will be conducted in our future studies to explain the relationship between mitophagy and skeletal muscle loss.

In conclusion, mitophagy is enhanced in the skeletal muscle of subjects with cancer cachexia. Inflammation and oxidative stress were also observed simultaneously. Overall, suppressing mitophagy could rescue mitochondrial function and skeletal muscle loss to a certain extent. Indeed, further research on mitophagy and cancer cachexia is essential to improve the outcomes of this patient population.

Author Contributions

ST and ZZ had equal contributions to this study. GW supervised the entire project. ST designed the study. ZZ, SL, YC, JW, HL, and MY performed study. ZZ and MY conducted data analyses. ZZ and ST wrote and revised the manuscript. All authors critically reviewed and approved the final manuscript.

Acknowledgments

Authors would like to thank all researchers and patients for the great cooperation and valuable contribution in this study. This study was funded by Shanghai "Rising Stars of Medical Talent" Youth Development Program ([2022]65), and Excellent Young Program of Zhongshan Hospital, Fudan University (2021ZSYQ14).

Conflict of Interest

No potential conflicts of interest were disclosed.

References

1 Fearon K, Strasser F, Anker SD, *et al*. Definition and classification of cancer cachexia: an international consensus. *Lancet Oncol* 2011; **12**: 489–495.
2 Schmidt SF, Rohm M, Herzig S, Berriel Diaz M. Cancer cachexia: more than skeletal muscle wasting. *Trends Cancer* 2018; **4**: 849–860.
3 Anandavadivelan P, Lagergren P. Cachexia in patients with oesophageal cancer. *Nat Rev Clin Oncol* 2016; **13**: 185–198.
4 Zhang Y, Wang J, Wang X, *et al*. The autophagic-lysosomal and ubiquitin proteasome systems are simultaneously activated in the skeletal muscle of gastric cancer patients with cachexia. *Am J Clin Nutr* 2020; **111**: 570–579.
5 Tardif N, Klaude M, Lundell L, Thorell A, Rooyackers O. Autophagic-lysosomal pathway is the main proteolytic system modified in the skeletal muscle of esophageal cancer patients. *Am J Clin Nutr* 2013; **98**: 1485–1492.
6 Glick D, Barth S, Macleod KF. Autophagy: cellular and molecular mechanisms. *J Pathol* 2010; **221**: 3–12.
7 Parzych KR, Klionsky DJ. An overview of autophagy: morphology, mechanism, and regulation. *Antioxid Redox Signal* 2014; **20**: 460–473.
8 Kitada M, Koya D. Autophagy in metabolic disease and ageing. *Nat Rev Endocrinol* 2021; **17**: 647–661.
9 Ashrafi G, Schwarz TL. The pathways of mitophagy for quality control and clearance of mitochondria. *Cell Death Differ* 2013; **20**: 31–42.
10 Bernardini JP, Lazarou M, Dewson G. Parkin and mitophagy in cancer. *Oncogene* 2017; **36**: 1315–1327.
11 Zhang J, Ney PA. Role of BNIP3 and NIX in cell death, autophagy, and mitophagy. *Cell Death Differ* 2009; **16**: 939–946.
12 Chen M, Chen Z, Wang Y, *et al*. Mitophagy receptor FUNDC1 regulates mitochondrial dynamics and mitophagy. *Autophagy* 2016; **12**: 689–702.
13 Manczak M, Kandimalla R, Yin X, Reddy PH. Mitochondrial division inhibitor 1 reduces dynamin-related protein 1 and mitochondrial fission activity. *Hum Mol Genet* 2019; **28**: 177–199.
14 Archer SL. Mitochondrial dynamics--mitochondrial fission and fusion in human diseases. *N Engl J Med* 2013; **369**: 2236–2251.
15 Favaro G, Romanello V, Varanita T, *et al*. DRP1-mediated mitochondrial shape controls calcium homeostasis and muscle mass. *Nat Commun* 2019; **10**: 2576.
16 Mao X, Gu Y, Sui X, *et al*. Phosphorylation of dynamin-related protein 1 (DRP1) regulates mitochondrial dynamics and skeletal muscle wasting in cancer cachexia. *Front Cell Dev Biol* 2021; **9**: 673618.
17 Wang J, Zhu P, Li R, Ren J, Zhou H. Fundc1-dependent mitophagy is obligatory to ischemic preconditioning-conferred renoprotection in ischemic AKI via suppression of Drp1-mediated mitochondrial fission. *Redox Biol* 2020; **30**: 101415.
18 Zhang Z, Chen Z, Liu R, *et al*. Bcl-2 proteins regulate mitophagy in lipopolysaccharide-induced acute lung injury via PINK1/Parkin signaling pathway. *Oxid Med Cell Longev* 2020; **2020**: 6579696.
19 He F, Huang Y, Song Z, *et al*. Mitophagy-mediated adipose inflammation contributes to type 2 diabetes with hepatic insulin resistance. *J Exp Med* 2021; **218**: e20201416.
20 Pradeepkiran JA, Reddy PH. Defective mitophagy in Alzheimer's disease. *Ageing Res Rev* 2020; **64**: 101191.
21 Lazarou M, Sliter DA, Kane LA, *et al*. The ubiquitin kinase PINK1 recruits autophagy receptors to induce mitophagy. *Nature* 2015; **524**: 309–314.
22 Lin Q, Li S, Jiang N, *et al*. Inhibiting NLRP3 inflammasome attenuates apoptosis in contrast-induced acute kidney injury through the upregulation of HIF1A and BNIP3-mediated mitophagy. *Autophagy* 2021; **17**: 2975–2990.
23 Aversa Z, Pin F, Lucia S, *et al*. Autophagy is induced in the skeletal muscle of cachectic cancer patients. *Sci Rep* 2016; **6**: 30340.
24 Kang EA, Park JM, Jin W, Tchahc H, Kwon KA, Hahm KB. Amelioration of cancer cachexia with preemptive administration of tumor necrosis factor-α blocker. *J Clin Biochem Nutr* 2022; **70**: 117–128.
25 Zhang Q, Song MM, Zhang X, *et al*. Association of systemic inflammation with survival in patients with cancer cachexia: results from a multicentre cohort study. *J Cachexia Sarcopenia Muscle* 2021; **12**: 1466–1476.
26 Martin L, Muscaritoli M, Bourdel-Marchasson I, *et al*. Diagnostic criteria for cancer cachexia: reduced food intake and inflammation predict weight loss and survival in an international, multi-cohort analysis. *J Cachexia Sarcopenia Muscle* 2021; **12**: 1189–1202.
27 Mizumura K, Cloonan SM, Nakahira K, *et al*. Mitophagy-dependent necroptosis contributes to the pathogenesis of COPD. *J Clin Invest* 2014; **124**: 3987–4003.
28 Bordt EA, Clerc P, Roelofs BA, *et al*. The putative Drp1 inhibitor mdivi-1 is a reversible mitochondrial complex I inhibitor that modulates reactive oxygen species. *Dev Cell* 2017; **40**: 583–594.e6.
29 Wang Y, Jasper H, Toan S, Muid D, Chang X, Zhou H. Mitophagy coordinates the mitochondrial unfolded protein response to attenuate inflammation-mediated myocardial injury. *Redox Biol* 2021; **45**: 102049.
30 Sliter DA, Martinez J, Hao L, *et al*. Parkin and PINK1 mitigate STING-induced inflammation. *Nature* 2018; **561**: 258–262.

doi: 10.3164/jcbn.23-1